Solid Earth Discuss., https://doi.org/10.5194/se-2017-94
Manuscript under review for journal Solid Earth
Discussion started: 24 August 2017

Solid Earth Discussions
Open Access
EGU

Rift zone-parallel extension during segmented fault growth: application to the evolution of the NE Atlantic

Alodie Bubeck[1], Richard. J. Walker[1], Jonathan Imber[2], Robert E. Holdsworth[2], Christopher J. MacLeod[3], David A. Holwell[1]

[1] Department of Geology, University of Leicester, Leicester, LE1 7RH, UK.
[2] Department of Earth Sciences, Durham University, Durham, DH1 3LE, UK.
[3] Department of Earth and Ocean Sciences, Cardiff University, Cardiff, CF10 3AT, UK.

Correspondence to: Alodie Bubeck (ab753@le.ac.uk)

Abstract. The mechanical interaction of propagating normal faults is known to influence the linkage geometry of first-order faults, and the development of second-order faults and fractures, which transfer displacement within relay zones. Natural examples of growth faults from two active volcanic rift zones (Koa'e, Big Island, Hawaii and Krafla, northern Iceland) illustrate the importance of relay zone heave gradients and associated vertical axis rotations in evolving continental rift systems. Detailed field mapping of deformation within two relay zones, located at the tips of en echelon rift faults, reveals pronounced heave displacement deficits that are accommodated by: (1) extensional-shear faults that strike at a low angle (<45°) to the main rift faults and accommodate components of both the regional extension and a rift zone–parallel extension; and (2) extension mode fractures that strike at a high angle (>45°) and accommodate a significant component of rift zone-parallel extension. Such extension parallel to the rift axis may oppose any shear-induced shortening that is typically required for vertical axis rotations (e.g. bookshelf faulting models). At the surface, this volume increase is accommodated by open fractures, but may be accommodated in the subsurface by veins or dikes oriented oblique- and normal to the rift axis. This proposal is consistent with data from exhumed contemporaneous fault and dike systems seen on the Faroe Islands and in Kangerlussuaq (East Greenland). Based on the findings presented here we propose a new conceptual model for the evolution of segmented continental rift basins on the NE Atlantic margins.

1 Introduction

Studies using natural examples and numerical or scaled-analogue modelling techniques have shown that normal faults grow through stages in which initially offset segments propagate towards each other and link to form composite structures (e.g. Trudgill and Cartwright, 1994 Gupta and Scholz, 2000; Peacock, 2002). The resulting mechanical interaction between fault segments can have an important influence on fault system evolution, including the geometry of first-order faults, and the development and distribution of second-order faults and fractures within developing inter-fault (relay) zones. Segmentation is a feature common to all scales of faults and fault development (e.g. Walsh et al., 2003; Long and Imber 2011) and the conservation of regional strain across networks of discontinuous segments has been well-established (e.g. Peacock and Sanderson, 1991; Peacock, 2002; Fossen and Rotevatn, 2016). Normal fault displacement is typically considered with emphasis on the vertical motion (fault throw), which can be measured using offset bedding, either in the field, laboratory or using high-resolution seismic imaging. In horizontally-layered materials, displacement (throw) gradients on adjacent coherent normal faults are commonly accommodated by relay structures (e.g., Peacock and Sanderson, 1991; Childs et al., 1995; Long and Imber, 2010), requiring horizontal axis bending of the host layering (Fig. 1). The bounding faults of a relay zone also exhibit opposing horizontal displacement (heave) gradients, which requires a component of vertical axis rotation to maintain the connection between the hanging wall and footwall (e.g. Ferrill and Morris, 2001). Few studies have addressed this rotational strain (see e.g., Koehn et al., 2008), and the resulting horizontal extension profile between faults or the potential for non-plane stresses and strains within the relay zone. Unlike horizontal axis rotation, it cannot be accommodated by layer-parallel or flexural slip between layers and thus requires the material to bend or stretch within the layer plane.

Here we present field examples of growth faults from two active volcanic rift zone segments - the Koa'e (Big Island, Hawai'i) and Krafla (northern Iceland) fault systems - to demonstrate the inherently three-dimensional (3D) strains

Solid Earth Discuss., https://doi.org/10.5194/se-2017-94
Manuscript under review for journal Solid Earth
Discussion started: 24 August 2017

associated with extensional strain gradients within evolving relay zones. The Koa'e fault system represents an early stage rift that connects the East and Southwest rift zones on the south flank of Kilauea Volcano to produce a continuous zone of extension that facilitates southward flank motion. The Krafla fissure swarm represents a well-established and highly extended portion of the Neo-Volcanic Zone of Iceland, a subaerially exposed segment of the NE Atlantic spreading ridge. The two case studies represent, respectively, early and advanced stages in normal fault linkage during rifting.

In both case studies the expression of surface strains records minor (≤20%) extension, in which respect they can be considered analogous to the surface expression of extensional systems in, for example, continental rifts. In neither case, however, do they provide insight into the deeper levels of rift systems. To assess what these strains may look like at greater crustal depths (e.g. ~1-3 km depth), and at a margin-scale, we also examine kinematic and geometric data for exhumed contemporaneous sets of faults and dikes along the Faroe Islands and Kangerlussuaq (East Greenland) portions of the NE Atlantic province. Based on these examples, we here suggest a new conceptual model for the evolution of segmented continental rift basins, with specific reference to the NE Atlantic margin.

2 Background

The primary, regional scale segmentation of extensional terranes is controlled by the development of networks of normal fault systems and the partitioning of strain across them. Normal faults comprise multiple discontinuous, non-collinear segments, with overlaps and segment linkage forming characteristic stepping geometries at a broad range of scales (e.g. Cartwright et al., 1996; Peacock et al., 2000; Acocella et al., 2005; Long and Imber, 2011). Two-dimensional analyses of the stresses surrounding en echelon faults and dikes have demonstrated that mechanical interaction of opposing elastic stress fields produce areas of highly perturbed stress, which exert a control on the growth, slip distribution and geometry of faults (e.g. Segall and Pollard, 1980; Sempere and Macdonald, 1986; Cowie and Scholz, 1992; Crider and Pollard, 1998). To maintain the extensional strain across the fault system as a whole (i.e. representing a coherent system), the volume ahead of the fault tips is required to accommodate the opposing along-strike displacement gradients on the bounding fault structures. Depending on the degree of overlap and separation of individual segments, this may lead to different styles of deformation (e.g. Tentler and Acocella, 2010) (Fig. 1a, b). This may be accommodated in this inter-fault region, or relay zone, through components of elastic and inelastic strain (e.g. Peacock and Sanderson, 1991, 1994; Childs et al., 1995; Long and Imber, 2010).

Using scaled-analogue models, Tentler and Acocella (2010) showed that a large underlap (relative to fracture length) between fracture segments produces elongate relay zones with new linking fractures opening ahead of the tips, striking sub-parallel to the bounding fractures (Fig. 1di). Decreasing the underlap of the bounding fractures (Fig. 1d, ii-iv) results in the growth of open fractures in the relay zones that strike at increasingly higher angles to the main structures. The propagation of these high angle fractures generate a local component of extension, and volume increase, in a direction parallel or at low angles to the strike of the bounding fractures. At the same time, the component of extension orthogonal to the bounding structures decreases. At larger overlap geometries (Fig. 1d, v), linking fractures strike at a lower angle, resulting in a reduction of the local component of bounding fracture-parallel extension and an increase in the fracture-normal component. The model configurations of Tentler and Acocella (2010) represent single stages of propagation and linkage, rather than the full progression. In nature, however, the process should graduate through some or all of these stages, as the bounding structures propagate toward each other and link, subjecting the relay zone to distortions as a function of the changing fault cut-off line lengths associated with slip accumulation (Fig. 1c,d).

It is typical to consider the distortions associated with normal fault displacement in terms of the vertical motion: the throw (e.g. Fig. 1d). This is perhaps due to the association of normal faults with gently dipping or horizontal bedding, which provides useful and abundant offset markers for measurement. There are fewer studies that have made detailed measurements of horizontal motions – the fault heave – due to the challenges in defining it accurately, particularly in seismic reflection datasets. Local deficits in fault throw, with respect to a coherent system, can be accommodated by the development of new synthetic faults in the relay zone, and/or by folding about a horizontal axis, producing the relay ramp. Any deficits in fault heave, on the other hand, require vertical axis rotation (Fig. 1c, e), which can be accommodated by the formation of new faults (i.e. hard-linkage: e.g. Gawthorpe and Hurst, 1993; Hus et al., 2006), or bending within the plane of bedding (i.e. soft-linkage: e.g. Childs et al., 1995; Faulds and Varga, 1998). At the surface, the evolution of such structural elements will have a profound influence on the evolving tectono-stratigraphic architecture of rift basins (e.g. Lambiase and

Solid Earth Discuss., https://doi.org/10.5194/se-2017-94
Manuscript under review for journal Solid Earth
Discussion started: 24 August 2017

Bosworth, 1995; Sharp et al., 2000; Hus et al., 2006) as well as contributing to the sealing potential or fluid flow properties of fault zones (e.g. Morley et al., 1990; Manzocchi et al., 2010; Seebeck et al., 2014).

In this paper we present new data for two normal fault systems exposed at the surface in active volcanic rift systems in Hawai'i and Iceland. We aim to demonstrate the importance of displacement variation as a function of fault heave, rather than throw, and highlight the potential for the development of local non-plane strains and volume change within relay zones. Surface-breaching normal faults in the Koa'e and Krafla fault systems cut sub-horizontal bedded lavas, which exhibit vertical columnar joint sets at a range of scales. Previous work has established that faults in layered basaltic sequences, at low confining pressures, develop as networks of extension fractures that open along favorably oriented pre-existing cooling joints in the lava pile, ahead of blind normal faults (e.g. Grant and Kattenhorn, 2004; Martel and Langley, 2006). Eventual linkage of fault and fracture networks at depth results in the development of surface-breaching, sub-vertical normal faults exhibiting components of horizontal and vertical displacement. The polygonal profile of columnar joints allows accurate measurement of regular piercing points in the horizontal plane, and therefore the accurate measurement of opening directions and magnitudes of extension fractures (no throw) and normal faults. Fault throw was also measured where applicable, but it should be noted that a majority of the structures encountered in the study areas are extension fractures that do not involve a shear component. This is typical of deformation patterns seen in many near surface rift zones (e.g. Grant and Kattenhorn, 2004; Casey et al., 2006).

3 Field study areas

3.1 The Koa'e fault system, Hawai'i

The Koa'e fault system is ~12 km long and ~3 km wide and is located on the south flank of Kilauea Volcano, the youngest intraplate volcanic system on Hawaii's Big Island. The Koa'e system connects two prominent rift zones: the Southwest and East Rift Zones, (SWRZ and ERZ: Fig. 2a) to form a near-continuous rift system that accommodates regional NNW-SSE extension (Dzurisin et al., 1984; Wright and Klein, 2006; Poland et al., 2012). Normal faults in the Koa'e fault system are subvertical and interpreted to be growth faults, associated with the forceful emplacement of dikes in the ERZ, the cumulative effect of which has been ~25-30 m of extension since the last volcanic resurfacing event 400-750 years ago (Duffield et al., 1975; Holcombe, 1987). Here we focus on a 3 km^2 area, ~5 km south of Kilauea's summit in the centre of the Koa'e fault system (Fig. 2a, b). Approximately 2000 measurements, covering three orders of length magnitude, were collected for: (1) extension fractures (hereafter, fracture), which develop in the footwalls of upward propagating normal faults (e.g. Martel and Langley, 2006); and (2) normal faults using differential GPS (dGPS) to record surface-breaching fault cut-off line positions at <10 cm horizontal resolution within the 3 km^2 area. Fractures were measured for strike and extension direction; aperture (the amount of opening measured normal to the plane) was also measured at several positions along each fracture.

Based on orientation, opening direction, and spatial association, we identify two dominant fault and fracture sets in the Koa'e fault system: (1) ENE-WSW (ERZ-parallel) striking fractures and normal faults that accommodate the regional NNW-SSE extension (sets A, C and D; Fig. 2b); and (2) NW-SE (ERZ-oblique) striking fractures that accommodate a more localised NE-SW extension (set B; Fig. 2b). The NW-SE (ERZ-oblique) striking fractures (set B) are restricted to a zone of underlap between two major ENE-WSW (ERZ-parallel) striking normal faults: sets A and C (Fig. 2 and 3). All measured fractures in this NW-SE striking set (set B) show purely extensional opening (Figure 2b), resulting in a local extension direction that is ~40° clockwise of the regional (NNW-SSE) extension. We found no evidence for cross-cutting relationships between ENE-WSW and NW-SE striking fracture sets (sets A, C and B, respectively, Fig. 2ci, ii). Unpublished measurements of ground cracks following the last major surface breaching event in the Koa'e (December 1965) identified fresh ENE-WSW striking extension fractures (here labelled set D: Fig. 2b, ciii; unpublished data courtesy of Don Swanson at the Hawaii Volcano Observatory), at which time fault and fracture sets A, B, and C had been mapped; we infer here that these existing sets either formed in a cyclic sequence, or formed contemporaneously.

The ENE-WSW striking sets comprise normal faults that dip to the north and demonstrate maximum throws of ~5-12 m, and footwall fractures with maximum apertures of ~4-5 m (sets A and C; Fig. 3). Individual surface-breaching normal fault segments show trace lengths of up to ~200 m, and exhibit discontinuous fault-parallel monoclinal flexures in fault hanging walls. Fault sets A and C (Fig. 2 and 3) are separated by ~800 m (measured in a NNW-SSE axis, parallel to the fault dip), and underlap by 200 m. The NW-SE striking fracture set are limited to this zone of underlap, and record smaller strains,

Solid Earth Discuss., https://doi.org/10.5194/se-2017-94
Manuscript under review for journal Solid Earth
Discussion started: 24 August 2017

with no surface-breaching fault segments, and fractures with trace lengths <200 m and apertures <2.5 m (set B: e.g. Fig. 3b). We infer here that this zone of underlap and separation represents a relay zone between fault sets A and C.

Figure 3 shows the summed surface extensional strains for each fracture set in the mapped area, as a function of the total plane-normal extension (i.e., extension measured in the dip azimuth), and the resolved contribution to NNW-SSE (regional) extension. Extension on set B fractures is in deficit compared to the surrounding regions with a total measured heave (aperture) peak of ~3.5 m compared to ~6 m for the northern bounding set A and 4.5 m for the southern bounding set C (Fig. 3b). A vertical displacement (throw) deficit is also recognized (Fig. 3c) from aerial LiDAR datasets with up to ~12 m of displacement measured across fault A and up to ~4 m across fault C and the monocline along fracture set B. The relative contributions of the components of rift zone-normal and rift zone-parallel extension also follow this distribution with a centrally located minimum of 3 m (rift zone-normal extension) on linking set B. This minimum is bound to the north by ~5 m of rift-normal extension on set A and ~4 m on set C to the south. Calculated rift zone-parallel extension is minor on southern bounding set C (up to 1.2 m) and peaks are approximately equal on the linking set B and northern bounding set A (up to 2.5 m). This suggests that although set B accommodates a component of rift zone-normal extension, this set contributes relatively little to the regional extensional strain as a whole. With no evidence for the relative timings of the bounding and linking fracture sets, simultaneous orthogonal extension directions have produced an area of inherently 3D strain within the relay zone. A kinematically and geometrically coherent fault array (e.g. Walsh et al., 2003) should exhibit an approximately centralized displacement maxima; this is not the case for horizontal (heave) displacement where we find a prominent extensional strain deficit in the centre of the array (Fig. 3b,c).

3.2 The Krafla fissure swarm, Iceland

Iceland sits at the junction between the northern termination of the Reykjanes Ridge, and the southern termination of the Kolbeinsey Ridge, with present-day rifting on the island accommodated by the Neo-Volcanic Zone. We focus here on the well-exposed Gjastykki valley, 10 km North of Krafla, within the Krafla fissure swarm (Fig. 4). Regional NW-SE extension in the Krafla fissure swarm is accommodated dominantly on surface-breaching normal faults with maximum throws of 10-30 m; monoclinal surface flexures occur as discontinuous structures in some fault hanging walls, but are rare compared to the Koa'e fault system. The focus of this study area is a relay zone surrounding the tips of en echelon rift zone-parallel normal faults that strike NNE-SSW (Fig. 4b, c).

Faults and footwall fractures in the Krafla system can be separated into three structural sets based on their kinematics and strike (Fig. 4c, d): (1) NNE-SSW striking (parallel to the rift axis: set A, B, C) fractures and normal faults, that accommodate rift zone-normal (WNW-ESE) extension; (2) NW-SE striking (rift-oblique: set A', B') normal faults and hybrid (extensional-shear) fractures that accommodate rift zone-oblique (ENE-WSW) extension; and (3) WNW-ESE striking (rift-normal: set D) fractures that accommodate rift zone-parallel (NNE-SSW) extension. NW-SE (set A',B') and WNW-ESE (set D) striking fractures are observed only in a zone of underlap ahead of two major rift-parallel normal faults (set A and B). Both of these sets are cut by a NNE-SSW striking normal fault showing up to 2 m of throw and set of fractures with up to 3 m of aperture (set B-C), which connect NW-SE striking sets B' and A' and accommodate rift zone-normal extension. The development of this set appears to form a link between rift-parallel sets B and C. Hence, rift-parallel striking faults and fractures, which cut, and are cut by, obliquely oriented sets, may represent the first and final stage of deformation in the rift zone, respectively (Fig. 4e). No consistent cross-cutting relationships are observed between rift-oblique and rift-normal striking structures (Fig. 4e), suggesting that they formed contemporaneously.

Figure 5 shows the summed extensional strains for each fracture set in the mapped area, as a function of the plane-normal extension, and the resolved contribution to WNW-ESE (regional) extension. Rift-oblique striking fault and fracture sets (set A', B': Fig. 4c, 5a) are well-developed and branch away from the tips of rift-parallel striking faults, with tensile openings of up to ~8 m (Fig. 5b) and estimated maximum throws of ~ 20 m. Rift-normal striking fractures (set D: Fig. 4c, 5a) represent the smallest strains in the relay zone with maximum fracture apertures of up to 2 m (Fig. 5b) and no vertical displacement (throw). Based on the total measured aperture profile (grey dotted line in Fig. 5b), the underlap zone does not appear to be in deficit compared to the surrounding regions, with an approximately centralized total aperture peak of ~14 m, compared to 8 m for southern bounding set B and 13.5 m for northern bounding sets A and C (Fig. 5b). When the directional

Solid Earth Discuss., https://doi.org/10.5194/se-2017-94
Manuscript under review for journal Solid Earth
Discussion started: 24 August 2017

components of this total measured extension are plot, however, we are able to define a pronounced heave deficit in the relay zone (blue and red dashed lines on Fig. 5b). Resolved rift zone-normal extension is greatest on northern bounding sets B and C (~12 m), followed by southern bounding set B (~10 m), with a low of ~9 m total aperture for linking fault and fracture sets (A', B', D, B-C: Figure 5b) in the overlap zone. Rift zone-parallel extension within the relay zone is significant for the area at ~ 8 m, compared to a maximum of 1 m for southern bounding set B and a maximum of 5.5 m for northern bounding sets A and C.

3.3 Summary and interpretations

Regional extension in the Koa'e and Krafla fault systems is accommodated by segmented rift zone-parallel faults that are discontinuous and underlapping at the present-day topographic surface. Relay zones, located at the lateral terminations of first-order segments, are characterized by second-order faults and fractures that strike oblique- and normal to the bounding rift faults and show a heave displacement deficit in the regional extensional strain (Figure. 3b and 5b). Fracture sets that strike at a low angle to the main rift zone (<45°) show extensional-shear opening (e.g. Krafla: Figure 4), and must therefore accommodate a combined rift zone-normal extension direction (i.e. contributing to the regional extension), and a component of rift zone-parallel shortening. Fracture sets that strike at high angles (i.e. >45°) to the main rift-parallel faults are dominantly tensile, and therefore provide a smaller contribution to the regional extension, but nevertheless represent a significant component of rift zone-parallel extensional strain. Observed rift-oblique extensional-shear fault and fracture sets are dominantly synthetic to each other, rather than bimodal (i.e., conjugate). As such, we infer that they facilitate a vertical axis rotation between the main rift faults, similar to a bookshelf-like faulting mechanism (Mandl, 1987). A bookshelf rotation about a vertical axis would involve a rift zone-normal material thickening, and must also involve a rift zone-parallel material thinning (cf. bookshelf rotations about a horizontal axis, which accommodate horizontal extension and vertical thinning). Fractures with strikes orthogonal to the main rift faults in the Krafla study area, however, display extensional openings that may counteract this shear-induced shortening, leading to an overall volume increase within the rift zone. At the surface, this volume increase is accommodated by open cracks, but may be accommodated in the subsurface by normal faults and dike emplacement oblique to, and normal to the rift axis.

4 Discussion

4.1 Rift zone-parallel extension associated with normal fault and rift systems

The potential for displacement transfer and locally anomalous (with respect to far-field stresses), three-dimensional strains during fault linkage has been recognized in field studies (e.g. Ferrill et al., 1999; Ferrill and Morris, 2001; Koehn et al., 2008, 2010; Morris et al., 2014), scaled analogue models (e.g. Tentler and Acocella, 2010; see Figure 1), and numerical simulations (e.g. Segall and Pollard, 1980; Crider and Pollard, 1998; Maerten et al., 2002). Such non-plane strains may be responsible for local instances of basin inversion, and reverse and strike-slip faulting in otherwise extensional regimes (e.g. Lin and Okubo, 2016; Sachau et al., 2016). The effect of horizontal heave displacement gradients requires vertical axis rotations (Ferrill and Morris, 2001), and may operate independently of scale (e.g. Morris et al., 2014), in the same manner as other fault characteristics. For instance, worldwide catalogues of relay zone geometry have demonstrated a power-law scaling relationship that covers approximately 8 orders of magnitude (e.g. Peacock, 2003; Long and Imber, 2011). Evidence for heave gradients and locally non co-axial strains are described at the at the tens of km separation scale in the East African Rift (e.g. Koehn et al., 2008, 2010; Sauchau et al., 2016) and the hundreds of km-scale in the Baikal rift zone (Hus et al., 2006) and the Hold With Hope relay zone in NE Greenland (Peacock et al., 2000). These examples show many characteristics similar to those observed in the Koa'e and Krafla study sites, including (1) segmented bounding faults; (2) progressive development of obliquely oriented ancillary fault structures internal to the relay zone that accommodate non-coaxial strains; and (3) rift zone-parallel connecting faults.

Evidence for vertical axis rotations at the rift zone scale (i.e. tens to hundreds of km) have previously been attributed to bookshelf-type faulting models (e.g. Green et al., 2014; Fig. 6a). In such models, a vertical axis rotation can contribute to rift zone-normal extension. In horizontal axis rotations, via bookshelf faulting, a shear couple in the vertical plane represents a horizontal extension, and a vertical shortening (i.e. crustal thinning). In vertical axis rotation, shortening would require a

Solid Earth Discuss., https://doi.org/10.5194/se-2017-94
Manuscript under review for journal Solid Earth
Discussion started: 24 August 2017

horizontal material thinning along the rift zone: In plane strain, this would not require vertical crustal thinning. Vertical axis rotations by this mechanism, with a shear couple in the horizontal plane therefore require horizontal shortening (Fig. 6). For a rigid block model, the rotation has the effect of causing a material thickening orthogonal to the rift zone (e.g. Fig. 1e). Figure 1e shows that this rotation also results in material extension parallel to the rift axis, allowing addition of new material as a volume increase; during non-rigid body rotations (e.g., Fig. 6), second-order faults may act to facilitate the coupled components of rift zone-normal extension and rift zone-parallel shortening (e.g., Fig. 6b). For faults in the Krafla study area we infer that rift zone-parallel shortening is counteracted, contemporaneously, by the extensional component of obliquely oriented extensional shear faults, and rift-normal striking extension fractures at the free surface (e.g., Fig. 6biii). At depth, this volume increase could occur as veins and/or dikes.

4.2 Is rift zone-parallel extension scale independent?

Heave gradients and the associated vertical axis rotations should result in extension parallel to the rift axis to compensate for rotation-related material thinning. Since rotations may occur across scales, we present a geometric and kinematic comparison between surface strains in the Koa'e and Krafla fault data, and upper crustal strains (~0-6 km) from the segmented rift basin systems along the NE Atlantic conjugate margins (Fig. 7a). Using new and published data for the Kangerlussuaq region (east Greenland margin) and Faroe Islands (European margin) we aim to consider whether a vertical axis rotation, driven by heave gradients, could serve as a viable explanation for margin-oblique and margin-normal striking structures that are hosted in basins along the NE Atlantic margins; we do not seek to directly compare the scale or regional dynamics of continental margins with volcanic island faulting or mid-ocean ridges, but rather the kinematic evolution of segmented fault systems. Our comparison is between the surface expression of fault sets (Koa'e and Krafla), and near-surface brittle deformations on the Atlantic margins. We do not seek here to address full crustal thickness stretching models.

The pre-break-up configuration of the NE Atlantic involved the development of offset spreading segments (the Reykjanes and Aegir systems; Fig. 7b-d) that accommodated a regional NW-SE extension, culminating in break-up and formation of the contiguous NE Atlantic (Gernigon et al., 2012). The Faroe Islands and Kangerlussuaq were located either side of the SW termination of the Aegir spreading ridge segment, and NE termination of the Reykjanes ridge segment, respectively (Fig. 7a), and both ridges record the initiation of oceanic spreading in the Early Ypresian (~55-53 Ma: Gernigon et al., 2012) (Fig. 7c). Prior to NE Atlantic spreading, the Faroes and Kangerlussuaq were located about 80 km apart (Ellis and Stoker, 2014). Both areas are dominated by Cenozoic North Atlantic Igneous Province lavas and intrusions, and both exhibit sequential deformation phases prior to, and contemporaneous with, Atlantic opening.

4.2.1 The Faroe Islands, European Atlantic margin

Deformation in the Faroe Islands (Fig. 8a) is characterized by sets of cross-cutting faults and intrusive igneous sheets that reflect reorientation of the local extension vector during and following emplacement of the Faroe Islands Basalt Group (57-54 Ma: Passey and Jolley, 2009; Fig. 7b). Based on fault and fracture geometry and kinematics (including paleostress analysis), together with cross-cutting relationships Walker et al. (2011) identified three main structural sets (Fig. 8c, d, e). These are (oldest to youngest): (1) N-S and NW-SE striking normal faults and dikes (margin-normal; Fig. 8c, ei) that accommodate E-W to NE-SW extension; (2) ENE-WSW to ESE-WNW conjugate dikes and strike-slip faults (margin-oblique; Figure 8c, d, eii) that accommodate N-S extension; and (3) NE-SW and NNE-SSW-striking strike-oblique-slip faults (margin-parallel; Fig. 8d, eiii) that accommodate NW-SE extension. Walker et al. (2011) interpreted the fault and intrusion sets as representing a progressive anti-clockwise rotation in the extension direction before, during and following continental break up. Set 1 (NW and N striking) faults are associated with thickness variations in the Faroe Islands Basalt Group (Passey and Jolley, 2009) suggesting that they are Paleocene in age. Using U-Pb geochronology for calcite-bearing fault rocks, Roberts and Walker (2016) showed that although dating of set 2 (ENE and ESE striking) faults suggest they are Mid-Eocene in age, there was potential for overlap with the ages of set 3 faults (Eocene and Miocene). Roberts and Walker (2016) were unable to constrain ages for set 1 faults, primarily due to high concentrations of common Pb, and very low U concentration. Margin-parallel (NE-SW striking) faults accommodate extension parallel to the regional extension (i.e. NW-SE). The apparently oldest structures strike NW-SE and are parallel to postulated margin-normal strike-slip (transfer) fault

Solid Earth Discuss., https://doi.org/10.5194/se-2017-94
Manuscript under review for journal Solid Earth
Discussion started: 24 August 2017

zones reported along the margin (e.g., Ellis et al., 2009). In the Faroe Islands, this set accommodates minor (~1%) extension parallel to the margins. The prevalent strain recorded on the Faroe Islands, in terms of distribution and scale of displacements, is associated with the phase of N-S extension, in which ENE-WSW and ESE-WNW conjugate dikes and strike-slip faults accommodate large lateral displacements (potentially up to hundreds of metres).

4.2.2. Kangerlussuaq, East Greenland Atlantic margin

Igneous activity in the Kangerlussuaq region of East Greenland (Fig. 9a), associated with continental break-up is thought to have occurred in three phases: 62-59 Ma, 57-54 Ma and 50-47 Ma (Tegner et al., 1998), with emplacement of the 7 km wide, layered gabbroic Skaergaard intrusion at ~56 Ma (Wotzlaw et al., 2012). As with the Faroe Islands, deformation is characterized by geometrically and temporally-linked suites of cross-cutting faults and dikes, hosted within the Archaean basement and Cretaceous-Cenozoic stratigraphy (Fig. 9b, c). Importantly, faults and dikes cut the Skaergaard intrusion, and compositionally similar macrodikes (e.g., the Miki Fjord macrodike: Fig. 9a, c) are thought to be contemporaneous with emplacement of the Skaergaard intrusion (Holm et al., 2006; Holwell et al., 2012), giving a well-constrained maximum age for the deformation. The ~500 m thick Miki Fjord macrodike strikes parallel to the margin and Reykjanes ridge segment (i.e., NE-SW; Fig. 9a, c), and accommodates margin-normal (NW-SE) extension. The macrodike is cut and offset by ESE-WNW oblique-extensional faults, which show lateral displacements of at least ~100 m (e.g. Fig. 9c), and form a conjugate set with ENE-WSW-striking faults that accommodate margin-oblique (N-S) extension (Fig. 9di). These faults also cut the Skaergaard intrusion (Fig. 9b) and strike parallel to conjugate dikes, with which they show a mutual cross-cutting relationship. Skaergaard additionally hosts margin-normal (N-S to NW-SE) faults and dikes, accommodating margin-parallel (NE-SW) extension (Fig. 9b, dii), which are cut by the margin-oblique structures (Fig. 9b). Locally, margin-parallel dikes are observed in the Skaergaard intrusion, which cut both of those sets (see also Irvine et al., 1998).

4.2.3. A vertical axis rotation model for the Faroe-Kangerlussuaq margins

Structures in the Faroe Islands and East Greenland share a common geometric, kinematic, and temporal evolution (Fig. 8 and 9), formed before, and during, continental break-up. The Faroe Islands sits atop a continental block (Bott, 1975), in an overlap region between the proto-Reykjanes and Aegir segments of the NE Atlantic (Ellis and Stoker, 2014); Kangerlussuaq sits on what is now the opposite conjugate margin. We propose that the geometry and kinematic development of structural sets can be compared with smaller scale structures that evolved in regions of extension deficit and rotation, such as the Koa'e and Krafla fault systems. Here we focus on the Krafla system, as the extensional strain accommodated there has produced surface breaching structures that are closely comparable to the Atlantic margin.

To make the comparison of relative fault orientations and kinematics between the Krafla analogue and the NE Atlantic margins, we have rotated the Krafla rift datasets into the orientation and overlap configuration of the Atlantic European margin basin systems: i.e. a NE-SW trending, right-stepping rift. Thus, a right-stepping mirror image of the left-stepping Krafla rift is used (Fig. 10a) and compared with the Reykjanes-Aegir system, with the rift-parallel striking faults rotated into parallelism with those of the NE Atlantic margin (Fig. 10b, c). Data rotation is undertaken in two ways here for comparison: (1) by rotating the measured planar data for the Krafla system into an orientation that matches the strike of basin- and sub-basin faults along the Faroe-Shetland Basin; and (2) by rotating the measured planar data for the Krafla system so that the average strike of the rift-parallel structures match the measured strike of rift-parallel structures in the Faroe Islands and East Greenland. The two styles of rotation result in a difference in second order fault orientation of 30°, which is significant for data comparison. However, both types of rotation lead to the second-order data becoming parallel with either ENE or ESE-striking structures mapped in the Faroe Islands and Kangerlussuaq (Fig. 11a-d). All of the study areas show kinematically near-identical fault sets, with a 20-28° spread in extension directions across datasets. Removing one or the other of the reoriented Krafla sets reduces the spread to 12-20°. Importantly, each dataset comprises: rift-parallel striking faults that open normal to the rift axis (red in Fig. 11e); rift-oblique striking structures that accommodate extension oblique to the rift zone (blue in Fig. 11e); rift-normal striking structures that accommodate extension parallel to the rift zone (yellow in Fig. 11e). Rift zone-parallel extension in the Krafla study area is accommodated by extension mode fractures at the surface that strike orthogonal to the bounding rift faults. Equivalent subsurface structural sets exposed in the Faroe Islands and in East Greenland are normal faults and dikes. Notably, evidence for this style of inter-rift system architecture

has also been noted in the East Africa Rift where, in younger portions of the rift, obliquely oriented dikes accommodate rift zone-parallel extension in the intervening relay zone between rift segments (tens of km scale: e.g. Muirhead et al., 2015).

Rift-parallel striking fault sets along both margins represent the first and final structural set. Timing relationships of fault sets on the Faroe Islands and in East Greenland imply a progressive vertical axis stress rotation at the regional scale, which is consistent with models that predict break-up involved a series of initially underlapping rift systems during rift propagation (Ellis and Stoker, 2014; Fig. 7b-d). Although the history of fault sets in the Krafla relay zone is less clear, the interpreted pattern fits well with the strains observed at a larger scale along the NE Atlantic margins (Fig. 11). We therefore propose that a vertical axis rotation model (associated with heave gradients) can account for margin-normal striking normal faults, dikes, and lineaments in segmented rift systems, and presents a viable alternative to a polyphase extension and reorganization, or strike-slip – *transfer* – models, that have been applied previously (e.g., Ellis et al., 2009). Our new model, however, cannot and should not be applied along the entire length of the European margin in a simple way. Along this margin segmentation styles vary considerably, from large-scale, localized transform faults, e.g. the Jan Mayan Fracture Zone, or the Senja Fracture Zone in the Norwegian-Greenland sea (e.g. Skogseid and Eldholm, 1987; Gernigon et al., 2009), to distributed, discontinuous continental style accommodation zones along the Møre-Faroes-Rockall portion of the margin.

Variations in the along-strike segmentation and scaling of fault populations have been well-documented in both continental rift (e.g. Hayward and Ebinger, 1996; Scholz and Contreras, 1998; Faulds and Varga, 1998) and oceanic fault populations (e.g. Carbotte and Macdonald, 1994; Macdonald, 1998). Variations have previously been attributed to changes in crustal thickness, strain rate (i.e. heat diffusion/magma supply), segment configuration, and the presence of pre-existing "weak" structures (e.g. Cowie, 1998; Corti et al., 2003; Tentler and Acocella, 2010; Gerya, 2012, 2013). Scaled-analogue models of normal fault populations have demonstrated that increases in effective elastic layer thickness results in a dominance of small and widely distributed faults (Ackermann et al., 1997, 2001). With increasing total extension, these authors noted that faults increased in number and length, producing a close and regularly spaced network. More recent scaled-analogue modeling of ridge-transform fault configurations also suggest that fault style and scaling is a function of strain rate and crustal thickness, with relatively thick lithosphere producing oblique zones of rifting and relatively thin lithosphere resulting in the development of transform faults that link the offset accreting segments (Gerya, 2012, 2013). With estimated crustal thicknesses in the NE Atlantic varying from ~3-10 km in the Norwegian-Greenland Sea to ~10-35 km in the Rockall Basin and the Greenland-Iceland-Faroes Ridge (Smallwood and White, 2002; Gernigon et al., 2009), variations in axis-parallel segmentation patterns are to be expected (e.g. Hayward and Ebinger, 1996). Localized and large-scale fracture zones along the NE Atlantic margins only occur where crustal thicknesses fall below 10 km, elsewhere we find thick crust and distributed fault systems that are dominated by accommodation zone-style stress transfer, rather than regional-scale strike-slip faults. The protracted extensional history of the region and superposition of NE Atlantic rifting on Paleozoic rift systems, themselves influenced by Caledonian and/or older fabrics, mean that pre-existing structural weaknesses are likely to be widespread along the margin (e.g. Doré et al., 1999), and the style of segmentation appears to vary considerably. Although the controls on segmentation style in the NE Atlantic are beyond the scope of this study to investigate, it is nevertheless important to consider the potential role of factors such as pre-existing structures, strain rate or crustal thickness when applying any single model to the entire margin.

5 Conclusions

- Discontinuous normal faults in the Koa'e and Krafla fault systems accommodate regional horizontal extensional strains via a combination of fault throw and heave on first-order rift faults, and by obliquely oriented second-order deformation, driven by heave displacement gradients and vertical axis block rotation within the intervening relay zones.

- Second-order deformation within the two studied relay zones accommodate components of the regional extension, but locally accommodate components of extension in a direction parallel to- and oblique to the rift zone.

- Locally heterogeneous fault populations within relay zones are attributed to locally non co-axial stress states associated with mechanical interaction and resulting fault displacement gradients rather than polyphase tectonic episodes.

- Relay zones are considered to be scale invariant characteristics in segmented extensional systems. Thus, we infer that vertical axis block rotations and the associated deformation, which accommodates deficits in fault heave, can operate at the rift system scale also.

- A displacement deficit-rotation model is applied to the NE Atlantic margins, in which host fault sets accommodate margin-parallel extension, and vertical axis rotation. We suggest that this is a viable alternative model to existing transfer fault zone models for the case study presented, but urge caution in applying the model along the length of a given system.

Author contribution. Data from Hawai'i and Iceland were collected by A. Bubeck. Data from the Faroe Islands and Greenland were collected by R. Walker. R. Holdsworth and J. Imber provided valuable discussion. C. MacLeod and D. Holwell assisted with data collection and contributed to the discussion. A. Bubeck prepared the manuscript with contributions from all co-authors.

Competing interests. The authors declare that they have no conflict of interest.

Acknowledgments

This study was funded via RJW's University of Leicester start-up fund, as part of AB's PhD project. Observations crucial to this study were made during RJW's PhD research, which was funded by Statoil (UK) Ltd. Thanks to Pierpaolo Guarnieri for making it possible to collect data in East Greenland, and the Føroya Dàtusavn for access to Faroes aerial imagery. We thank Richard England for discussions during manuscript preparation. We also thank Don Swanson and Mike Poland at HVO, Hawai'i, for their help and advice during fieldwork planning and data collection, and the National Park Service for granting a research permit to conduct fieldwork in the Koa'e fault system.

References

Ackermann, R. V., & Schlische, R. W. (1997). Anticlustering of small normal faults around larger faults. Geology, 25 (12).

Ackermann, R. V., Schlische, R. W., & Withjack, M. O. (2001). The geometric and statistical evolution of normal fault systems: an experimental study of the effects of mechanical layer thickness on scaling laws. Journal of Structural Geology, 23, 1803-1819.

Acocella, V., Morvillo, P., & Funiciello, R. (2005). What controls relay ramps and transfer faults within rift zones? Insights from analogue models. Journal of Structural Geology, 27(3), 397-408. doi:10.1016/j.jsg.2004.11.006.

Bott, M. H. P. (1975). Structure and evolution of the north Scottish shelf, the Faeroe block and the intervening region. Petroleum and the continental shelf of North-west Europe, 1, 105-115.

Bürgmann, R., & Pollard, D. (1994). Slip distributions on faults: effects of stress gradients, inelastic deformation, heterogeneous host-rock stiffness, and fault interaction. Journal of Structural Geology, 16(12), 1675-1690.

Carbotte, S. M., & Macdonald, K. C. (1994). Comparison of seafloor tectonic fabric at intermediate, fast, and super fast spreading ridges: Influence of spreading rate, plate motions, and ridge segmentation on fault patterns. Journal of Geophysical Research: Solid Earth, 99(B7), 13609-13631. doi:10.1029/93jb02971.

Cartwright, J., Mansfield, C. S., & Trudgill, B. (1996). The growth of normal faults by segment linkage. In P. G. Buchanan & D. A. Nieuland (Eds.), Modern Developments in Structural Interpretation, Validation and Modelling. (Vol. Geological Society Special Publication No. 99). London, UK: The Geological Society.

Casey, M., Ebinger, C., Keir, D., Gloaguen, R., & Mohamed, F. (Eds.). (2006). Strain accommodation in transitional rifts: extension by magma intrusion and faulting in Ethopian rift magmatic segments. Geological Society, London, Special Publications, Vol. 259. The Geological Society of London.

Childs, C., Watterson, J., & Walsh, J. J. (1995). Fault overlap within developing normal fault systems. Journal of the Geological Society, London, 152, 535-549.

Corti, G., Bonini, M., Conticelli, S., Innocenti, F., Manetti, P., & Sokoutis, D. (2003). Analogue modelling of continental extension: a review focused on the relations between the patterns of deformation and the presence of magma. Earth-Science Reviews, 63(3-4), 169-247. doi:10.1016/s0012-8252(03)00035-7.

Cowie, P. (1998). Normal fault growth in three-dimensions in continental and oceanic crust. In W. R. Buck, P. T. Delaney, J. A. Karson, & Y. Lagabrielle (Eds.), Faulting and magmatism at mid-ocean ridges. Washington, D.C. American Geophysical Union. doi:10.1029/GM106p0027.

Cowie, P. A., & Scholz, C. H. (1992). Physical explanation for the displacement-length relationship of faults using a post-yield fracture mechanics model. Journal of Structural Geology, 14(10), 1133-1148. doi:10.1016/0191-8141(92)90065-5.

Crider, J. G., & Pollard, D. D. (1998). Fault linkage: Three-dimensional mechanical interaction between echelon normal faults. Journal of Geophysical Research, 103(B10), 24373. doi:10.1029/98jb01353.

Doré, A. G., Lundin, E. R., Birkeland, O., Eliassen, P. E., & Jensen, L. N. (1997). The NE Atlantic margin; implications of late Mesozoic and Cenozoic events for hydrocarbon prospectivity. Petroleum Geoscience, 3(2), 117-131. doi:10.1144/petgeo.3.2.117.

Doré, A. G., Lundin, E. R., Jensen, L. N., Birkeland, Ø., Eliassen, P. E., & Fichler, C. (1999). Principal tectonic events in the evolution of the northwest European Atlantic margin. 41-61. doi:10.1144/0050041.

Doré, A. G., Lundin, E. R., Kusznir, N. J., & Pascal, C. (2008). Potential mechanisms for the genesis of Cenozoic domal structures on the NE Atlantic margin: pros, cons and some new ideas. Geological Society, London, Special Publications, 306(1), 1-26. doi:10.1144/sp306.1.

Duffield, W. A. (1975). Structure and Origin of the Koae Fault System, Kilauea Volcano, Hawaii. Geological Survey Professional Paper (856).

Dzurisin, D., Koyanagi, R. Y., & English, T. T. (1984). Magma supply and storage at Kiluea Volcano, Hawaii, 1956-1983. Journal of Volcanology and Geothermal Research, 21, 177-206.

Ellis, D., & Stoker, M. S. (Eds.). (2014). The Faroe-Shetland Basin: a regional perspective from the Paleocene to the present day and its relationship to the opening of the North Atlantic Ocean. In S.J.C. Cannon and D. Ellis (Eds), Hydrocarbon exploration to exploitation West of Shetlands. Geological Society, London, Special Publications (Vol. 397). The Geological Society of London.

Ellis, D., Passey, S. R., Jolley, D. W., & Bell, B. R. (2009). Transfer zones: the application of new geological information from the Faroe Islands applied to the offshore exploration of intra and sub-basalt strata. Paper presented at the Faroe Islands exploration conference: proceedings of the 2nd conference, Torshavn, Faroe Islands.

Faulds, J. E., & Varga, R. J. (1998). The role of accommodation zones and transfer zones in the regional segmentation of extended terranes. In J. E. Faulds & J. H. Stewart (Eds.), Accommodation zones and transfer zones: the regional segmentation of the Basin and Range Province: Boulder, Colorado (Vol. 323): Geological Society of America Special Paper.

Ferrill, D. A., & Morris, A. P. (2001). Displacement gradient and deformation in normal fault systems. Journal of Structural Geology, 23, 619-638.

Ferrill, D. A., Stamatakos, J. A., & Sims, D. (1999). Normal fault corrugation: implications for growth and seismictiy of active normal faults. Journal of Structural Geology, 21, 1027-1038.

Fossen, H., & Rotevatn, A. (2016). Fault linkage and relay structures in extensional settings—A review. Earth-Science Reviews, 154, 14-28. doi:10.1016/j.earscirev.2015.11.014.

Gaina, C., Gernigon, L., & Ball, P. (2009). Palaeocene-Recent plate boundaries in the NE Atlantic and the formation of the Jan Mayen microcontinent. Journal of the Geological Society, 166(4), 601-616. doi:10.1144/0016-76492008-112.

Gawthorpe, R. L., & Hurst, J. M. (1993). Transfer zones in extensional basins: their structural style and influence on drainage development and stratigraphy. Journal of the Geological Society, 150(6), 1137-1152. doi:10.1144/gsjgs.150.6.1137.

Gernigon, L., Gaina, C., Olesen, O., Ball, P. J., Péron-Pinvidic, G., & Yamasaki, T. (2012). The Norway Basin revisited: From continental breakup to spreading ridge extinction. Marine and Petroleum Geology, 35(1), 1-19. doi:10.1016/j.marpetgeo.2012.02.015.

Gerya, T. (2012). Origin and models of oceanic transform faults. Tectonophysics, 522-523, 34-54. doi:10.1016/j.tecto.2011.07.006.

Gerya, T. V. (2013). Initiation of transform faults at rifted continental margins: 3D petrological-thermomechanical modeling and comparison to the Woodlark Basin. Petrology, 21(6), 550-560. doi:10.1134/s0869591113060039.

Grant, J. V., & Kattenhorn, S. A. (2004). Evolution of vertical faults at an extensional plate boundary, southwest Iceland. Journal of Structural Geology, 26(3), 537-557. doi:10.1016/j.jsg.2003.07.003.

Green, R. G., White, R. S., & Greenfield, T. (2014). Motion in the north Iceland volcanic rift zone accommodated by bookshelf faulting. Nature Geoscience, 7, 29-33. doi:10.1038/ngeo201210.1038/NGEO2012.

Gupta, A., & Scholz, C. H. (2000). A model of normal fault interaction based on observations and theory. Journal of Structural Geology, 22, 865-879.

Hayward, N. J., & Ebinger, C. J. (1996). Variations in the along-axis segmentation of the Afar Rift system. Tectonics, 15(2), 244. doi:10.1029/95tc02292.

Holcombe, R. T. (1987). Eruptive history and long-term behaviour of Kilauea Volcano. In R. W. Decker, T. L. Wright, & P. H. Stauffer (Eds.), Volcanism in Hawaii (Vol. 1): US Geological Survey Professional Paper.

Holm, P. M., Heaman, L. M., & Pedersen, L. E. (2006). Baddeleyite and zircon U–Pb ages from the Kærven area, Kangerlussuaq: Implications for the timing of Paleogene continental breakup in the North Atlantic. Lithos, 92(1-2), 238-250. doi:10.1016/j.lithos.2006.03.035.

Holwell, D. A., Abraham-James, T., Keays, R. R., & Boyce, A. J. (2012). The nature and genesis of marginal Cu–PGE–Au sulphide mineralisation in Paleogene Macrodykes of the Kangerlussuaq region, East Greenland. Mineralium Deposita, 47(1-2), 3-21. doi:10.1007/s00126-010-0325-4.

Hus, R., De Batist, M., Klerkx, J., & Matton, C. (2006). Fault linkage in continental rifts: structure and evolution of a large relay ramp in Zavarotny; Lake Baikal (Russia). Journal of Structural Geology, 28(7), 1338-1351. doi:10.1016/j.jsg.2006.03.031

Irvine, T. N., Andersen, J. C. Ø., & Brooks, C. K. (1998). Geological Society of America Bulletin, 110(11), 1398. doi:10.1130/0016-7606(1998)110<1398:ibabwb>2.3.co;2.

Koehn, D., Aanyu, K., Haines, S., & Sachau, T. (2008). Rift nucleation, rift propagation and the creation of basement micro-plates within active rifts. Tectonophysics, 458(1-4), 105-116. doi:10.1016/j.tecto.2007.10.003.

Koehn, D., Lindenfeld, M., Rümpker, G., Aanyu, K., Haines, S., Passchier, C. W., & Sachau, T. (2010). Active transsection faults in rift transfer zones: evidence for complex stress fields and implications for crustal fragmentation processes in the western branch of the East African Rift. International Journal of Earth Sciences, 99(7), 1633-1642. doi:10.1007/s00531-010-0525-2.

Lambiase, J. J., & Bosworth, W. (1995). Structural controls on sedimentation in continental rifts. In J. J. Lambiase (Ed.), Hydrocarbon habitat in rift basins (Vol. Geological Society Special Publications No. 80). London, UK: The Geological Society.

Lin, G., & Okubo, P. G. (2016). A large refined catalog of earthquake relocations and focal mechanisms for the Island of Hawai‘i and its seismotectonic implications. Journal of Geophysical Research: Solid Earth. doi:10.1002/2016jb013042.

Long, J. J., & Imber, J. (2010). Geometrically coherent continuous deformation in the volume surrounding a seismically imaged normal fault-array. Journal of Structural Geology, 32(2), 222-234. doi:10.1016/j.jsg.2009.11.009.

Long, J. J., & Imber, J. (2011). Geological controls on fault relay zone scaling. Journal of Structural Geology, 33(12), 1790-1800. doi:10.1016/j.jsg.2011.09.011.

Macdonald, K. C. (1998). Linkages between faulting, volcanism, hydrothermal activity and segmentation on fast spreading centers. In W. R. Buck, P. T. Delaney, J. A. Karson, & Y. Lagabrielle (Eds.), Faulting and magmatism at mid-ocean ridges. Washington, D.C.: American Geophysical Union. doi:10.1029/GM106p0027.

Maerten, L., Gillespie, P., & Pollard, D. D. (2002). Effects of local stress perturbation on secondary fault development. Journal of Structural Geology, 24, 145-153.

Mandl, G. (1987). Tectonic deformation by rotating parallel faults: the "bookshelf" mechanism. Tectonophysics, 141, 277-316.

Manzocchi, T., Childs, C., & Walsh, J. J. (2010). Faults and fault properties in hydrocarbon flow models. Geofluids. doi:10.1111/j.1468-8123.2010.00283.x.

Martel, S. J., & Langley, J. S. (2006). Propagation of normal faults to the surface in basalt, Koae fault system, Hawaii. Journal of Structural Geology, 28(12), 2123-2143. doi:10.1016/j.jsg.2005.12.004.

Morley, C. K., Nelson, R. A., Patton, T. I., & Munn, S. G. (1990). Transfer zones in the East Africa Rift System and their relevance to hydrocarbon exploration in rifts. The American Association of Petroleum Geologists Bulletin, 74(8), 1234-1253.

Morris, A. P., McGinnis, R. N., & Ferrill, D. A. (2014). Fault displacement gradients on normal faults and associated deformation. AAPG Bulletin, 98(6), 1161-1184. doi:10.1306/10311312204.

Muirhead, J. D., Kattenhorn, S. A., & Le Corvec, N. (2015). Varying styles of magmatic strain accommodation across the East African Rift. Geochemistry, Geophysics, Geosystems, 16(8), 2775-2795. doi:10.1002/2015gc005918.

Passey, S. R., & Jolley, D. W. (2009). A revised lithostratigraphic nomenclature for the Palaeogene Faroe Islands Basalt Group, NE Atlantic Ocean. Earth and Environmental Science Transactions of the Royal Society of Edinburgh, 99(3-4), 127. doi:10.1017/s1755691009008044.

Peacock, D. C. P. (2002). Propagation, interaction and linkage in normal fault systems. Earth Science Reviews, 58, 121-142.

Peacock, D. C. P. (2003). Scaling of transfer zones in the British Isles. Journal of Structural Geology, 25(10), 1561-1567. doi:10.1016/s0191-8141(03)00008-7.

Peacock, D. C. P., & Sanderson, D. J. (1991). Displacements, segment linkage and relay ramps in normal fault zones. Journal of Structural Geology, 13(6), 721-733.

Peacock, D. C. P., & Sanderson, D. J. (1994). Geometry and Development of Relay Ramps in Normal Fault Systems. AAPG Bulletin, 78. doi:10.1306/bdff9046-1718-11d7-8645000102c1865d.

Peacock, D. C. P., Price, S. P., Whitham, A. G., & Pickles, C. S. (2000). The World's biggest relay ramp: Hold With Hope, NE Greenland. Journal of Structural Geology, 22, 843-850.

Poland, M. P., Miklius, A., Sutton, A. J., & Thornber, C. R. (2012). A mantle-driven surge in magma supply to Kilauea Volcano during 2003-2007. Nature Geoscience, 5. doi:10.1038/ngeo1426.

Roberts, N. M. W., & Walker, R. J. (2016). U-Pb geochronology of calcite-mineralized faults: Absolute timing of rift-related fault events on the northeast Atlantic margin. Geology, G37868.37861. doi:10.1130/g37868.1.

Sachau, T., Koehn, D., Stamps, D. S., & Lindenfeld, M. (2016). Fault kinematics and stress fields in the Rwenzori Mountains, Uganda. International Journal of Earth Sciences, 105(6), 1729-1740. doi:10.1007/s00531-015-1162-6.

Scholz, C. H., & Contreras, J. C. (1998). Mechanics of continental rift architecture. Geology, 26(11), 967-970.

Seebeck, H., Nicol, A., Walsh, J. J., Childs, C., Beetham, R. D., & Pettinga, J. (2014). Fluid flow in fault zones from an active rift. Journal of Structural Geology, 62, 52-64. doi:10.1016/j.jsg.2014.01.008.

Segall, P., & Pollard, D. D. (1980). Mechanics of Discontinuous Faults. Journal of Geophysical Research, 85(B8), 4337-4350.

Sempere, J. C., & Macdonald, K. C. (1986). Overlapping spreading centers: implications from crack growth simulation by the displacement discontinuity method. Tectonics, 5(1), 151-163.

Sharp, I. R., Gawthorpe, R. L., Underhill, J. R., & Gupta, S. (2000). Fault-propagation folding in extensional settings: Examples of structural style and synrift sedimentary response from the Suez rift, Sinai, Egypt. Geological Society of America Bulletin, 112(12), 1877-1899. doi:10.1130/0016-7606.

Skogseid, J., & Eldholm, O. (1987). Early Cenozoic crust at the Norwegian continental margin and the conjugate Jan Mayen Ridge. Journal of Geophysical Research: Solid Earth, 92(B11), 11471-11491. doi:10.1029/JB092iB11p11471.

Smallwood, J. R., & White, R. S. (2002). Ridge-plume interaction in the North Atlantic and its influence on continental breakup and seafloor spreading. In D. W. Jolley & B. R. Bell (Eds.), The North Atlantic Igneous Province: Stratigraphy, Tectonic, Volcanic and Magmatic Processes (Vol. 197, pp. 15-37). London, UK: The Geological Society of London.

Tegner, C., Duncan, R. A., Bernstein, S., Brooks, C. K., Bird, D. K., & Storey, M. (1998). 40Ar-39Ar geochronology of Tertiary mafic intrusions along the East Greenland rifted margin: Relation to flood basalts and the Iceland hotspot track. Earth and Planetary Science Letters, 156, 75-88.

Tentler, T., & Acocella, V. (2010). How does the initial configuration of oceanic ridge segments affect their interaction? Insights from analogue models. Journal of Geophysical Research, 115(B1). doi:10.1029/2008jb006269.

Trudgill, B., & Cartwright, J. (1994). Relay-ramp forms and normal fault linkages. Canyonlands National Park, Utah. Geological Society of America Bulletin, 106, 1143-1157.

Walker, R. J., Holdsworth, R. E., Imber, J., & Ellis, D. (2011). Onshore evidence for progressive changes in rifting directions during continental break-up in the NE Atlantic. Journal of the Geological Society, 168(1), 27-48. doi:10.1144/0016-76492010-021.

Walsh, J. J., Bailey, W. R., Childs, C., Nicol, A., & Bonson, C. G. (2003). Formation of segmented normal faults: a 3D perspective. Journal of Structural Geology, 25(1251-1262).

Wotzlaw, J. F., Bindeman, I. N., Schaltegger, U., Brooks, C. K., & Naslund, R. H. (2012). High-resolution insights into episodes of crystallization, hydrothermal alteration and remelting in the Skaergaard intrusive complex. Earth and Planetary Science Letters, 355-356, 199-212. doi:10.1016/j.epsl.2012.08.043.

Wright, T. L., & Klein, F. W. (2006). Deep magma transport at Kilauea volcano, Hawaii. Lithos, 87(1-2), 50-79. doi:10.1016/j.lithos.2005.05.004.

Solid Earth Discuss., https://doi.org/10.5194/se-2017-94
Manuscript under review for journal Solid Earth
Discussion started: 24 August 2017

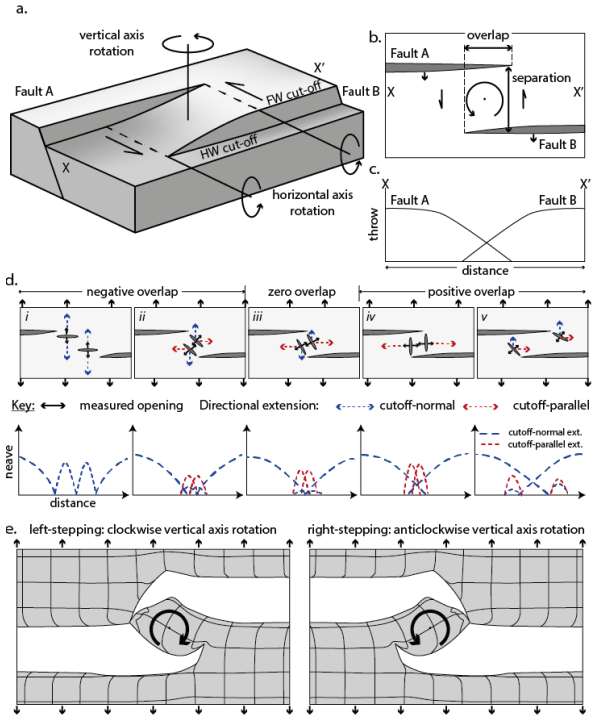

Figure 1. (a) Schematic diagram illustrating a relay zone between two normal faults (after Ferrill and Morris, 2001); (b) Map view of the block model in (a) showing fault overlap and separation; (c) Distance versus displacement (throw) profile for transect X-X'; (di-v) Second-order fault geometries as a function of fault overlap (redrawn from Tentler and Acocella, 2010) with local and regional extension directions indicated. Graphs show schematic displacement (heave)-length plots for the bounding fractures and linking geometries shown; (e) Modelled strain fields and rotation ahead of two left- and right-stepping en echelon open-mode fractures (redrawn from Tentler and Acocella, 2010).

Solid Earth Discuss., https://doi.org/10.5194/se-2017-94
Manuscript under review for journal Solid Earth
Discussion started: 24 August 2017

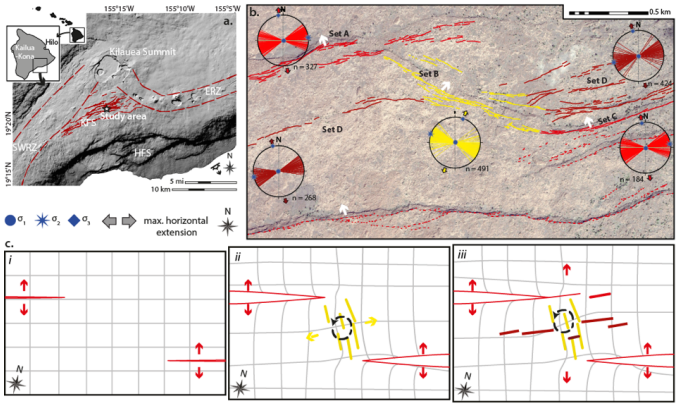

Figure 2. (a) Simplified structural elements map of Kilauea Volcano's south flank, showing the study area within the Koa'e fault system (KFS); ERZ: East Rift Zone; SWRZ: Southwest Rift Zone; HFS: Hilina Fault System. Inset shows position of A, on the south coast of Big Island, Hawaii; (b) WorldView image of the study area showing mapped fractures. White arrows indicate fault dip directions. Lower hemisphere stereographic projections indicate mapped fracture orientations and observed extension directions. Dashed lines are not included in this analysis; (c) Proposed evolution of fault sets: (i) propagation of the main rift-fault set (set A and C); (ii) interaction between sets A and C produces deficits of heave displacement, requiring vertical axis block rotation in the relay zone, and local reorientation of extension direction (set B); (iii) development of new rift-parallel structures (set D).

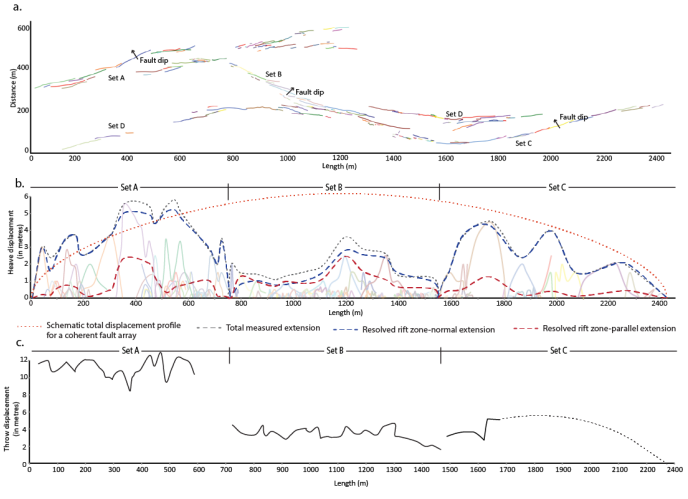

Figure 3. (a) Distribution of mapped fractures in the study area; (b) Profile of horizontal displacement (heave) vs length for mapped fractures. Dotted grey line indicates cumulative aperture for each set. Dashed blue lines indicate the calculated component of rift zone-normal extension on each fracture set. Dashed red lines indicate the calculated component of rift zone-parallel extension on each fracture set. Dotted orange line represents a hypothetical total displacement profile for a

Solid Earth Discuss., https://doi.org/10.5194/se-2017-94
Manuscript under review for journal Solid Earth
Discussion started: 24 August 2017

single fault (e.g. Gupta and Scholz, 2000), or a kinematically and geometrically coherent fault array (e.g. Walsh et al., 2003) where the maximum displacement is located centrally along the fault, or array; (c) Profile of estimated vertical displacement (throw) vs length for segments of surface-breaking faults. No evidence for throw was identified along NW-SE striking fractures of set B.

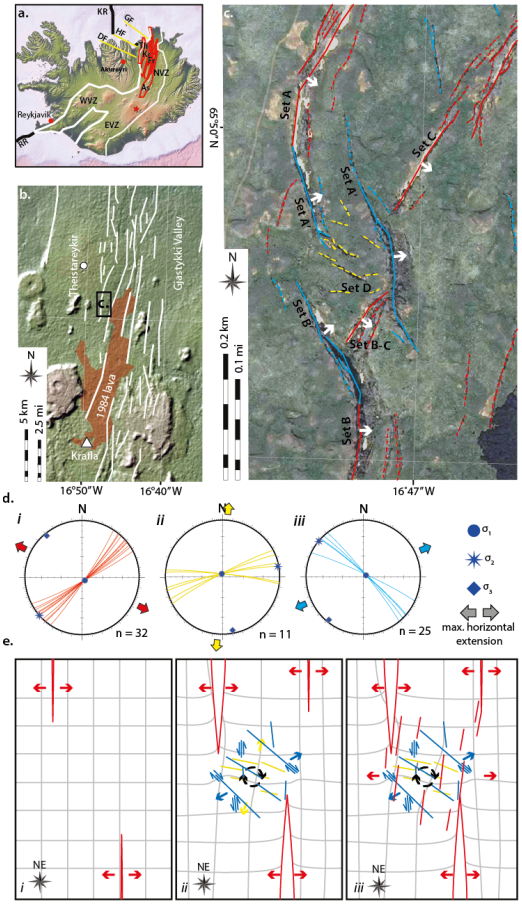

Figure 4. (a) Map of Iceland highlighting the major tectonic elements: Reykjanes Ridge (RR); the Kolbeinsey Ridge (KR); South Iceland Seismic Zone (SISZ); West Volcanic Zone (WVZ); East Volcanic Zone (EVZ); Neo-Volcanic Zone (NVZ: the axial rift zone); Askja volcanic centre (As); Fremri-Namur volcanic centre (Fr); Krafla volcanic centre (Kr); Theistareykir volcanic centre (Th); the Tjörnes Fracture Zone (TFZ) comprising the Dalvik lineament (DF), the Husavik-Flatey Fault (HF) and the Grimsey lineament (GF); (b) Location of study area in the Gjastykki Valley within the Krafla fissure swarm. White arrows indicate dip direction for fault scarps in the area; (c) Mapped structures in the study area, color-coded based on orientation and kinematics: (1) rift zone-parallel faults and fractures (red); (2) rift zone-oblique faults and fractures (blue); and (3) rift zone-normal fractures (yellow); (d) Lower hemisphere stereographic projections showing measured extension directions for each of the three structural sets; (e) Proposed evolution of fault sets: (i) Propagation of the main rift-fault sets A and B; (ii) interaction between sets A and B leads to a horizontal displacement deficit and vertical axis block rotation in the relay zone, and induced local reorientation of extension direction accommodated on variably oriented ancillary faults and fractures; (iii) continued propagation of the main rift faults (A, B and C) leads to the development of new rift-parallel structures.

Solid Earth Discuss., https://doi.org/10.5194/se-2017-94
Manuscript under review for journal Solid Earth
Discussion started: 24 August 2017

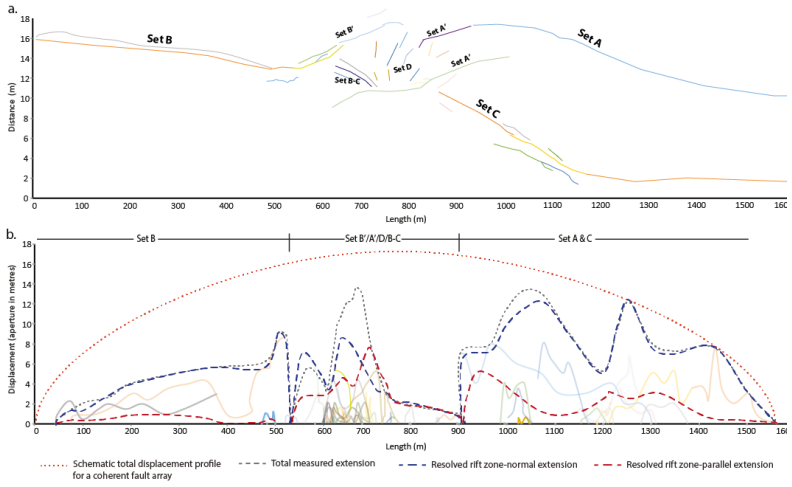

Figure 5. (a) Distribution of mapped faults and fractures in the study area; (b) Profile of horizontal displacement (heave) vs length for mapped fractures. Dotted grey line indicates the total measured aperture for structures in each set. Dashed blue lines indicate the calculated component of extension on each fracture set that occurs in a direction orthogonal to the rift zone. Dashed red lines indicate the calculated component of extension on each fracture set that occurs in a direction parallel to the rift zone. Extension across the system as a whole is represented by a hypothetical displacement profile for a single fault or kinematically and geometrically coherent fault array (dotted orange line).

Solid Earth Discuss., https://doi.org/10.5194/se-2017-94
Manuscript under review for journal Solid Earth
Discussion started: 24 August 2017

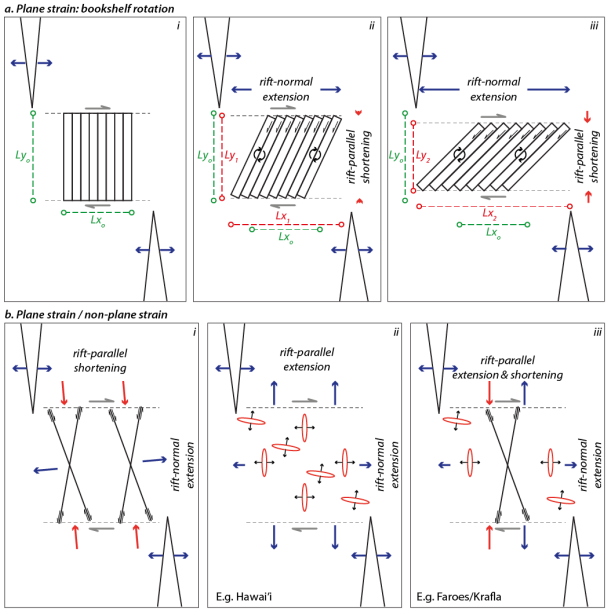

Figure 6. Horizontal plane 2D conceptual models for inter-fault/inter-rift relay rotation. (a) Bookshelf rotation model showing (i-iii) progressive rotation leading to rift normal extension, and rift-parallel shortening; (b) Schematic models for structures observed in the study areas presented here: (i) conjugate extensional shear faults, (ii) extension fractures, and (iii) a combination of extension fractures and conjugate extensional shear faults. If faults develop throw, as in the Krafla example, the system becomes non-plane strain. Models are not to scale.

Solid Earth Discuss., https://doi.org/10.5194/se-2017-94
Manuscript under review for journal Solid Earth
Discussion started: 24 August 2017

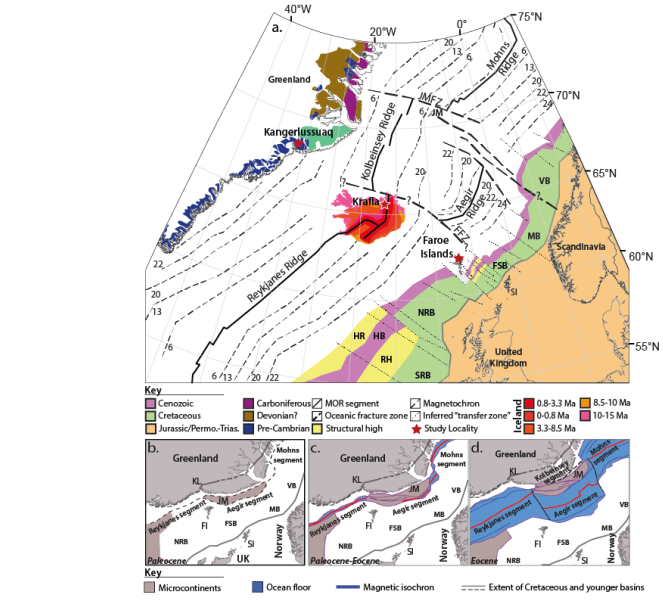

Figure 7. (a) NE Atlantic tectonic elements map: Hatton Rise (HR), Hatton Basin (HB), Rockall High (RH), South Rockall Basin (SRB), North Rockall Basin (NRB), Faroe-Shetland Basin (FSB), Shetland Islands (SI), Møre Basin (MB), Vøring Basin (VB), Jan Mayan (JM), Jan Mayan Fracture Zone (JMFZ), Tjörnes Fracture Zone (TFZ), Faroes Fracture Zone (FFZ). Map was compiled using: basin ages from Doré et al., (1997); oceanic magnetic anomalies from Gaina et al. (2009); Iceland stratigraphic ages from Doré et al. (2008). Study localities indicated by stars; (b-d) Schematic model for a segmented opening of the NE Atlantic during the Paleogene (after Ellis and Stoker, 2014). Faroe Islands (FI); Kangerlussuaq (KL).

Solid Earth Discuss., https://doi.org/10.5194/se-2017-94
Manuscript under review for journal Solid Earth
Discussion started: 24 August 2017

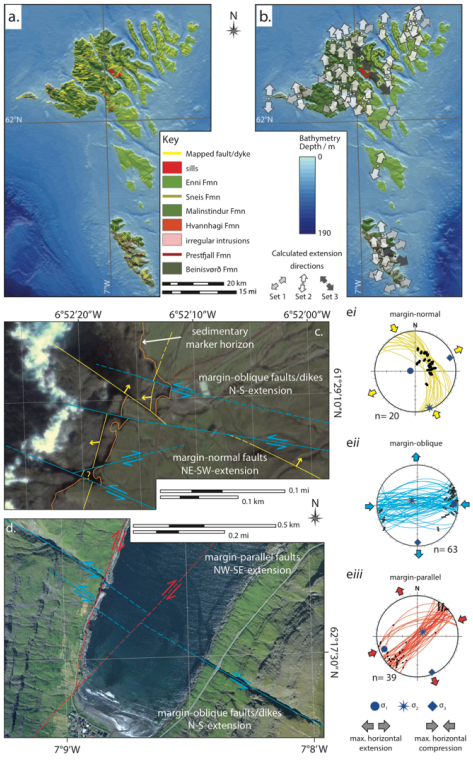

Figure 8. (a) Onshore structural element map of the Faroe Islands; (b) Inferred extension directions indicating an island-wide anticlockwise rotation in extension direction through time; (c) Margin-oblique faults cut margin-normal faults; (d) Margin-parallel faults cut rift-oblique faults and dikes; (e) Lower hemisphere stereographic projections for relative-age-constrained examples of the three main fault sets observed.

Solid Earth Discuss., https://doi.org/10.5194/se-2017-94
Manuscript under review for journal Solid Earth
Discussion started: 24 August 2017

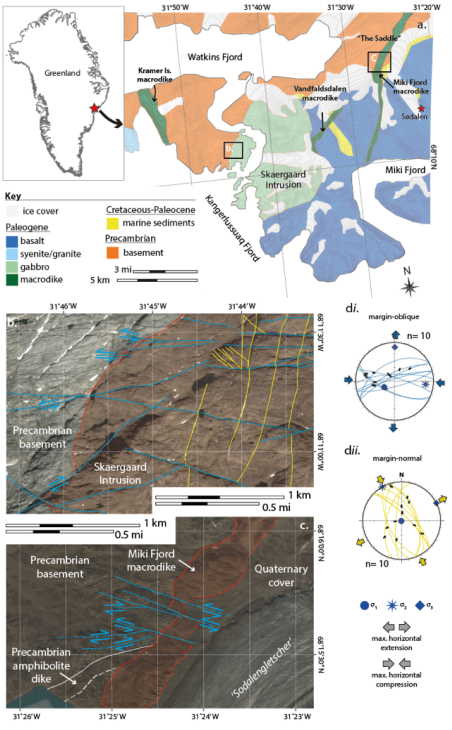

Figure 9. (a) Geological map of the Skaergaard intrusion and surrounding area (redrawn from Holwell et al., 2012). Contours indicate 50 m elevation intervals from sea level; (b) Margin-normal striking faults and dikes cut the Skaergaard intrusion, which are in turn cut by margin-oblique striking faults and dikes; (c) Margin-oblique striking faults cut the margin-parallel Miki Fjord macrodike; (d) Lower hemisphere stereographic projections for relative-age-constrained examples of the three main fault sets observed.

Solid Earth Discuss., https://doi.org/10.5194/se-2017-94
Manuscript under review for journal Solid Earth
Discussion started: 24 August 2017

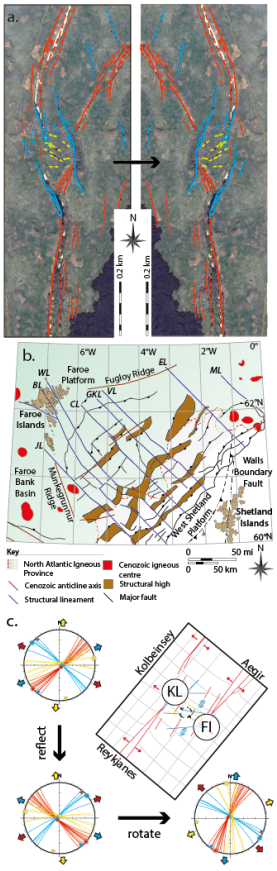

Figure 10. (a) Reflection of left-stepping Krafla faults to a right-stepping NE Atlantic rift configuration; (b) Map of the European margin of the NE Atlantic showing the broad NE-SW basin trend. JL: Judd Lineament; CL: Clare Lineament; GKL: Grimur Kamban Lineament; VL: Victory Lineament; EL: Erlend Lineament; ML: Møre Lineament; BL: Brynhild Lineament; WL: Westray Lineament; (c) Krafla faults are rotated into the orientation of the Atlantic European margin basin system and compared with the Reykjanes-Aegir system.

Solid Earth Discuss., https://doi.org/10.5194/se-2017-94
Manuscript under review for journal Solid Earth
Discussion started: 24 August 2017

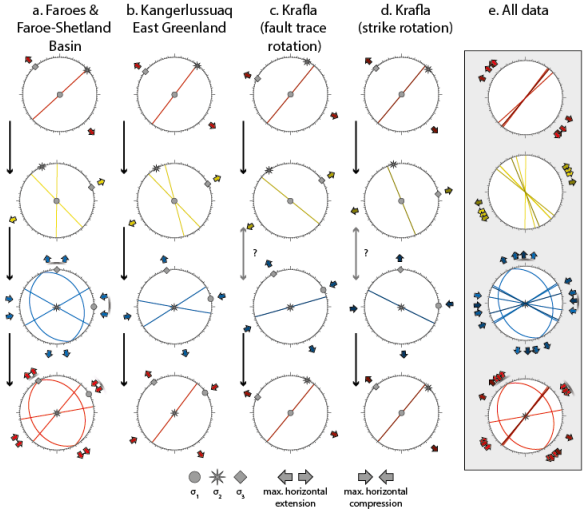

Figure 11. Comparison of averaged structural orientations and kinematics for the Faroe Islands (a) and East Greenland (b); (c) Krafla data is reflected and rotated so that the surface traces match the NE Atlantic basin system; (d) Krafla data is reflected and rotated so that the measured planar data matches the measured data from the NE Atlantic basin system; (e) Combined summary of orientations and kinematics from each study area.